

Accelerating Stochastic Quantum Chemistry

Verena A. Neufeld* and Alex J. W. Thom*

Department of Chemistry, Lensfield Road, Cambridge CB2 1EW, United Kingdom

E-mail: verena.a.neufeld@gmail.com; ajwt3@cam.ac.uk

Abstract

The convergence of full configuration interaction quantum Monte Carlo (FCIQMC) is accelerated using a quasi-Newton propagation (QN) which can also be applied to coupled cluster Monte Carlo (CCMC). The computational scaling of this optimised propagation is $\mathcal{O}(1)$, keeping the additional computational cost to a bare minimum. Its effects are investigated deterministically and stochastically on a model system, the uniform electron gas, with Hilbert space size up to 10^{40} and shown to accelerate convergence of the instantaneous projected energy by over an order of magnitude in the FCIQMC test case. Its capabilities are then demonstrated with FCIQMC on an archetypal quantum chemistry problem, the chromium dimer, in an all-electron basis set with Hilbert space size of about 10^{22} yielding highly accurate FCI energies.

1 Introduction

Accurate energies of electronic systems are not only crucial as benchmarks and verification for other, often computationally cheaper, methods (see e.g. Refs. 1–4) but are also needed when knowledge of those energies to a very high accuracy and precision is desired, for example when determining the low-energy crystal/molecular structures (e.g. 5–7) or vibrational spectra (e.g. Refs. 8–10). Wavefunction based quantum chemistry methods, such as (full) configuration interaction, (F)CI, 11,12 or coupled cluster theory, CC, 1,13–15 can give ac-

curate, if not exact, energies. This accuracy is systematically improvable unlike density functional theory 16,17 and they do not require *ab initio* knowledge of the wavefunction as diffusion Monte Carlo 18 does. Coupled cluster at the level of singles doubles and perturbative triples, CCSD(T), 19 has been shown to be able to give chemical accuracy, 1 kcal/mol, in some systems and is said to be the “gold standard”. 1

In the last decade, Booth et al. 20 and Thom 21 introduced highly parallelisable 22,23 stochastic versions of FCI, FCIQMC, and CC, CCMC, respectively, reducing memory costs and thus enabling calculations at larger basis sets. Not just molecules have been tackled with FCIQMC and CCMC (e.g. see Refs. 21–31), but also the uniform electron gas 31–37 or realistic solids 38,39 for example. Besides accurate ground state energies, FCIQMC has given excited state energies as well. 40–44 Some of its great benefits were demonstrated when FCIQMC reached systems of extremely large Hilbert space sizes using the initiator approximation, 22,33,45 and other improvements of the algorithms have further increased the sampling efficiency of FCIQMC and/or CCMC, 23,27,46–49 with a recent diagrammatic CCMC version increasing efficiencies by moving CCMC closer to conventional coupled cluster. 50

An irksome problem faced by FCIQMC and CCMC has not yet been largely discussed in the literature: the computational effort to reach equilibration can be very significant and thus it can take a prohibitive amount of time before the energy can be even roughly estimated. Here, we introduce a modification to the algorithms: the quasi-Newton method which is

commonly used in conventional deterministic coupled cluster.⁵¹ This is closer to using the quadratically convergent Newton–Raphson optimisation to reach equilibration instead of the linearly convergent steepest descent method. The Hessian required may be approximated by using inexpensive Fock expectation value sums. Since this method has been developed and implemented^{39,1} for CCMC and FCIQMC, Blunt et al.⁵² have also introduced an alternative Jacobi pre-conditioned propagation.⁵³ A comparison is made to their method which is computationally more expensive than the approach presented here. Note that other propagator improvements, which are not discussed here, exist, including the use of Chebyshev expansion⁵⁴ and techniques used in the machine learning community which have also been applied to Quantum Monte Carlo methods to accelerate convergence.^{55–57} Deustua et al.^{58,59} have used FCIQMC and CCMC to estimate deterministic amplitudes/coefficients and managed to converge to highly accurate energies quickly doing so, see for example the CAD-FCIQMC method.⁵⁹ This approach is orthogonal to the convergence acceleration shown here, in fact they can be most likely employed simultaneously to improve convergence.

First, we will describe the quasi-Newton propagation, followed by analysing its convergence behaviour in both *deterministic* and *stochastic* propagations and comparing it to the original, Jacobi, and full Newton propagations. Finally, the quasi-Newton propagation is applied to the chromium dimer in the full Ahlrichs’ SV basis⁶⁰ demonstrating its capabilities for accurate calculations of large quantum chemical systems.

2 Theory

The quasi-Newton propagation formalism is derived by treating FCIQMC as an optimisation problem. The derivation is similar to a derivation by Davidson.⁵³ The conclusion also holds for CCMC. Past literature^{20,21,23,31,39,45} contains detailed descriptions of the CCMC and

FCIQMC algorithms.

In FCIQMC, the lowest eigenvalue of the Hamiltonian is found along with an approximation of its eigenvector which is the ground state wavefunction. Working in Slater determinant space, the ground state wavefunction can be written as $\Psi_0 = \sum_{\mathbf{i}} c_{\mathbf{i}} |\mathbf{D}_{\mathbf{i}}\rangle$ where \mathbf{i} is a unique label for (known) determinant $|\mathbf{D}_{\mathbf{i}}\rangle$ and its corresponding (unknown) coefficient $c_{\mathbf{i}}$ that is determined using FCIQMC. The constraint is the normalisation of the wavefunction, $\langle \Psi | \Psi \rangle = N$ for some constant N . A Lagrangian \mathcal{L} with Lagrange multiplier E can therefore be written as

$$\mathcal{L} = \langle \Psi | \hat{H} | \Psi \rangle - E(\langle \Psi | \Psi \rangle - N). \quad (1)$$

Differentiating gives the gradient

$$g_{\mathbf{i}} = \frac{\partial \mathcal{L}}{\partial c_{\mathbf{i}}^*} \propto \langle \mathbf{D}_{\mathbf{i}} | \hat{H} - E | \Psi \rangle. \quad (2)$$

Setting $\mathbf{g}=\mathbf{0}$ gives the converged (F)CI equations $\langle \mathbf{D}_{\mathbf{i}} | \hat{H} - E | \Psi \rangle = 0$ for all \mathbf{i} . In the original FCIQMC formalism,²⁰ $g_{\mathbf{i}} = \langle \mathbf{D}_{\mathbf{i}} | \hat{H} - E | \Psi \rangle$ is used to propagate from the initial guess to the ground state wavefunction in imaginary time, τ , with an update equation equivalent to steepest descent,

$$\mathbf{c}(\tau + \delta\tau) = \mathbf{c}(\tau) - \delta\tau \mathbf{g}(\tau) \quad (3)$$

using time step $\delta\tau$. The optimised wavefunction is Ψ_0 with energy E .

Steepest gradient descent approaches the solution linearly and is therefore inefficient. The quadratically convergent Newton–Raphson method propagates the coefficients towards $\mathbf{g}=\mathbf{0}$ by

$$\mathbf{c}(\tau + \delta\tau) = \mathbf{c}(\tau) - \delta\tau \tilde{\mathbf{H}}^{-1} \mathbf{g}(\tau) \quad (4)$$

where the time step $\delta\tau$ was retained for extra flexibility. The elements of the Hessian $\tilde{\mathbf{H}}$ are given by

$$\tilde{H}_{\mathbf{ij}} = \frac{\partial g_{\mathbf{i}}}{\partial c_{\mathbf{j}}} \propto \langle \mathbf{D}_{\mathbf{i}} | \hat{H} - E | \mathbf{D}_{\mathbf{j}} \rangle. \quad (5)$$

Since inverting $\tilde{\mathbf{H}}$ is highly expensive, approximations to $\tilde{\mathbf{H}}^{-1}$ are necessary. It may be as-

¹See <https://github.com/hande-qmc/hande> for code.

sumed that the off-diagonal elements in $\tilde{\mathbf{H}}$ are not very significant compared to the diagonal elements and so can be set to zero, leaving an easily invertible diagonal matrix, provided no diagonal elements are zero. Davidson⁶¹ has noted the connection of pre-conditioning to the Newton–Raphson algorithm; while derived differently, this is equivalent to the Jacobi pre-conditioned propagation used by Blunt et al.⁵²

Here, the example of coupled cluster theory is followed⁵¹ where Fock expectation values for orbitals i , $\langle i|\hat{F}|i\rangle$, are used in an approximation to the diagonal Hamiltonian elements and off-diagonal elements are ignored. The diagonal elements of $\tilde{\mathbf{H}}$, $\propto \langle D_j|\hat{H} - E_{\text{HF}} - E_{\text{proj.}}|D_j\rangle$, are approximated by the sum of Fock expectation values of occupied orbitals in D_j minus the sum of Fock expectation values of occupied orbitals in the reference,

$$\langle D_j|\hat{H} - E|D_j\rangle \approx \sum_{m \text{ in } j} \langle m|\hat{F}|m\rangle - \sum_{m' \text{ in } 0} \langle m'|\hat{F}|m'\rangle. \quad (6)$$

Note that the computational cost of Blunt’s Jacobi pre-conditioned propagation⁵² is at least $\mathcal{O}(N_{\text{el.}})^2$ whereas the computational cost due to the quasi-Newton propagation is $\mathcal{O}(1)$.

3 Deterministic Propagation

To test this approximation, the different propagation techniques were first deterministically tested on a small model system where the true eigenvalues and eigenvectors were known, and stochastic noise, reaching the level of a sufficient number of particles and other challenges in stochastic propagations, could be ignored so

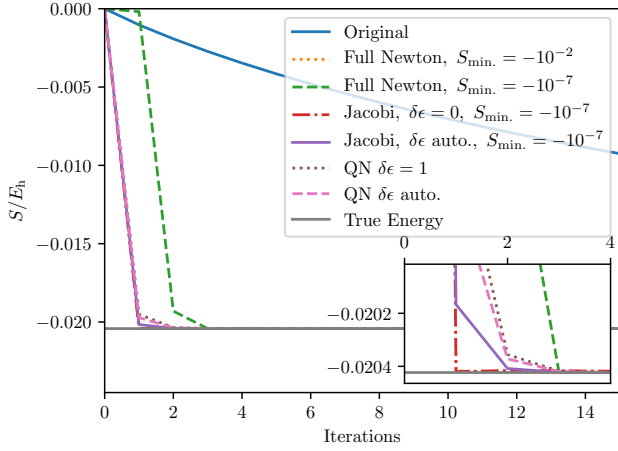
²To approximate $\tilde{\mathbf{H}}$, we need to evaluate $\langle D_j|\hat{H} - E|D_j\rangle$ as part of the death step for any type of propagation, so there is no extra cost in the death step. For the spawn step, $\langle D_i|\hat{H} - E|D_i\rangle$ is needed. Since D_i and D_j differ by at most a double excitation, $\langle D_j|\hat{H} - E|D_j\rangle$ can be used as a starting point and the difference can be calculated. This is an $\mathcal{O}(N_{\text{el.}})$ operation (Personal communication with Dr. Nick Blunt).

the focus was solely on how many iterations were needed to converge.

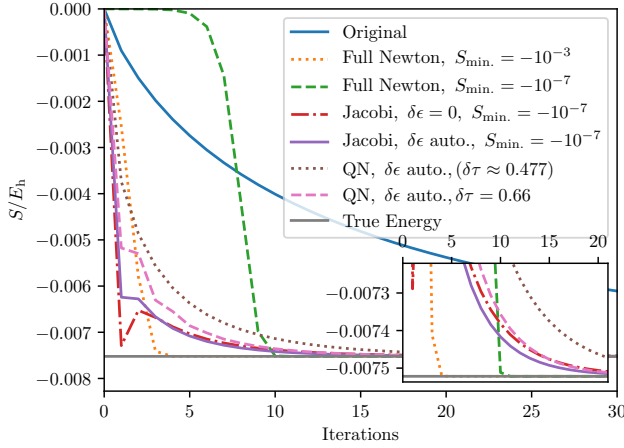
The model system studied was the three-dimensional uniform electron gas (UEG) with two electrons of opposite spin in 1850 spinorbitals which has a Hilbert space size of 925. There, the Fock value for spinorbital m is given by⁶²

$$\langle m|\hat{F}|m\rangle = \frac{1}{2}|\mathbf{k}|^2 - \sum_{\substack{n \text{ in } 0 \\ m \neq n \\ \text{same spin}}} \left\langle nm \left| \frac{1}{r_{12}} \right| mn \right\rangle \left(+ \frac{1}{2} V_{\text{Mad.}} \right) \quad (7)$$

where the last term in round brackets including the Madelung constant per electron $V_{\text{Mad.}}$ is added to spinorbitals m occupied in the reference only. $V_{\text{Mad.}} \approx -2.837297 \times (\frac{3}{4\pi r_s^3 N_{\text{el.}}})^{1/3}$ as determined by Schoof et al.^{63,64} with Wigner-Seitz radius r_s . Using the HANDE QMC code,³⁹ an FCI calculation was performed and Hamiltonian matrix elements were calculated. The initial guess for the wavefunction was a vector with 1 at the D_0 position and 0 otherwise. This corresponds to a standard FCIQMC calculation with initially one Monte Carlo particle at the reference determinant. The shift S was set to the projected energy at every iteration. The time step was set to the reciprocal of the highest eigenvalue of $\mathbf{A}^{-1}\tilde{\mathbf{H}}$ where in the original propagation \mathbf{A} is the identity and in the other propagations it is the Hessian $\tilde{\mathbf{H}}$ or an approximation thereof. This was inspired by the fact that the highest allowed time step in FCIQMC is twice the reciprocal of the highest eigenvalue of $\tilde{\mathbf{H}}$ ^{20,65} although this might not apply to all propagations exactly. The full Newton propagation used a Hessian with elements $\langle D_i|\hat{H} - 0.99S|D_j\rangle$ with a factor of 0.99 since its inverse would otherwise tend to be singular as $S \rightarrow E_{\text{corr.}}$. In the first iteration, where the shift and projected energy are zero, the first diagonal element is set to a small number such as 10^{-2} , 10^{-3} or 10^{-7} (see figure 1), in the case of the full Newton and Jacobi propagations. If *auto.* mode is chosen when using the quasi-Newton propagation, the first diagonal element



(a) Propagation for $r_s = 0.5a_0$.



(b) Propagation for $r_s = 20a_0$.

Figure 1: Deterministic propagation of the 3D UEG with two electrons of opposite spins in 1850 spinorbitals with original, full Newton, Jacobi preconditioned and quasi-Newton propagation for $r_s = 0.5a_0$ (a) and $r_s = 20a_0$ (b). Jacobi $\delta\epsilon$ auto. sets the first diagonal element of the approximated Hessian to its second element whereas $\delta\epsilon = 0$ leaves the diagonal untouched. The shift is set to the projected energy at each iteration and the time step (except for the quasi-Newton run with $\delta\tau = 0.66$) for each propagation is the reciprocal of the highest eigenvalue of the propagation matrix $\mathbf{A}^{-1}\tilde{\mathbf{H}}$. In case of full Newton and Jacobi propagations, $S = S_{\min.}$ if $|S| < |S_{\min.}|$. The full Newton curve with $S_{\min.} = -10^{-2}$ and the Jacobi one with $\delta\epsilon = 0$ cannot be distinguished at this scale.

of the approximated Hessian would be zero, so it is set to the second diagonal element. When using the Jacobi propagation, E in the propagation is set to the shift S and a threshold $\delta\epsilon$ is applied or the first element set to the second (auto. $\delta\epsilon$). Figure 1 shows the propagation for $r_s = 0.5a_0$ and $r_s = 20a_0$. For quasi-Newton, two time steps are shown; one found as described above (≈ 0.477), and the other being 0.66 which is higher.

Clearly, in terms of convergence with respect to iterations, the original propagation is outperformed by the others which perform similarly to each other. As demonstrated by the full Newton propagation the initial guess for $S = S_{\min.}$ can obviously affect convergence. The higher time step used for quasi-Newton performs slightly better than the automatically found time step but it is still similar in behaviour. The more correlated the UEG system gets, the higher r_s , the smaller the range in Fock eigenvalues so the more similar the original propagation is to the quasi-Newton propagation.

4 Stochastic Propagation

Next, the quasi-Newton propagation is compared with the original propagation in FCIQMC. The quasi-Newton propagation can be straightforwardly implemented into FCIQMC as the only changes are in the *spawn* and *death* steps. In the case of the *spawn* step, the probability that a spawn is accepted is divided by Δ_i where

$$\Delta_i = \begin{cases} \Delta'_i & \text{if } \Delta'_i \geq \delta\epsilon \\ \Delta_v & \text{otherwise} \end{cases} \quad (8)$$

with

$$\Delta'_i = \sum_{m \text{ in } j} \langle m | \hat{F} | m \rangle - \sum_{m' \text{ in } 0} \langle m' | \hat{F} | m' \rangle. \quad (9)$$

$\delta\epsilon$ is a threshold and Δ_v an alternative value chosen which could be set to 1 (see later part on the chromium dimer) or, as in this stochastic UEG study here, to $\delta\epsilon$. Similarly to the deterministic investigation, $\delta\epsilon$ can be chosen to be

the difference between the sum of Fock energies of the reference and first excited determinant to maximise the time step possible. In the original *death* step, the *death* probability of a particle on determinant $|D_i\rangle$ is written as²⁰

$$p_{\text{death}}(|D_i\rangle) \propto \delta\tau \langle D_i | \hat{H} - S | D_i \rangle. \quad (10)$$

If a quasi-Newton modification were also performed to the *death* step, the resulting *death* probability would be $\frac{p_{\text{death}}(|D_i\rangle)}{f_i}$. We consider the hypothetical case where the estimate of the wavefunction is a multiple of the true wavefunction, but S is not equal to the true energy the wavefunction would stay at the true solution as all determinants are affected equally by the error in S in the *death* step. However, in the case of quasi-Newton, due to the determinant dependence of Δ_i , the estimate of the wavefunction would move away from the true solution. A modified *death* step (inspired by the coupled cluster Monte Carlo modification of Franklin et al.⁶⁶) is

$$p_{\text{death}}(|D_i\rangle) \propto \delta\tau \left(\frac{\langle D_i | \hat{H} - E_{\text{proj.}} | D_i \rangle}{\Delta_i} + \rho(E_{\text{proj.}} - S) \right), \quad (11)$$

with the projected energy $E_{\text{proj.}}$ and ρ as a constant population control factor to add an extra degree of freedom. We have assumed that E_{HF} has already been subtracted of the Hamiltonian matrix diagonal. At the true solution, $E_{\text{proj.}}$ takes the correct value so the net effect of the first term in equation 11 when applied to the whole population is zero, and the latter term merely scales the whole population, so the wavefunction remains at the true solution.

Using the spin non-polarised three dimensional (3D) UEG again, this time with 1850 spinorbitals, 14 electrons, and $r_s = 0.5a_0$, the stochastic propagations using FCIQMC with quasi-Newton and the original propagation were compared. The instantaneous projected energies were binned with respect to the cumulative number of particles, $N_{\text{tot.}}$, to reach those instantaneous projected energies and the mean in each bin for each calculation run cal-

culated. The same calculation was then run at least 20 times with different random number generator seeds. The means of these independent bin means are shown in figure 2 with their standard deviations and standard errors across the different runs as error bars. Empty bins did not contribute to the mean or its errors. The bin positions are the same for all calculations. Note that not all calculations ran for the same number of iterations, some ended early. The cumulative number of particles $N_{\text{tot.}}$ is a measure of the cost of the calculation that is more implementation- and platform-independent than the compute time for example, as an iteration in the FCIQMC algorithm scales approximately linearly in the number of particles at that time step³. A pre-calculated $\mathcal{O}(1)$ version of a *uniform Power-Pitzer* excitation generator adapted to the UEG was used.^{48,67} Floating-point amplitudes^{46,68} were employed with a spawn cutoff of 0.01. Figure 2 shows that the instantaneous projected energy converges significantly faster when using the quasi-Newton propagation. The time steps for the quasi-Newton propagation are 10–40 times greater than time steps of the original propagations shown. $\delta\epsilon \approx 11.8E_h$, the Fock value difference between the ground and first excited determinant of the same symmetry. As expected, using a lower initial population decreases the initial cost of converging to a certain energy but increases the noise. Population control has not been applied here, we have just focussed on convergence, not evaluating the final energy.

To test how the system size affects the performance of quasi-Newton compared to the original propagation, i.e. whether quasi-Newton can be (even) more beneficial in larger systems, the convergence for the same 3D uniform electron gas but with 11150 spinorbitals was investigated and compared to the 1850 spinorbitals case shown in figure 2. This is a system with Hilbert space size of about 10^{40} . The memory capacity of the spawn array was fixed and calculations were allowed to increase their population until this array was full and the calcu-

³Each particle does one spawn attempt here.

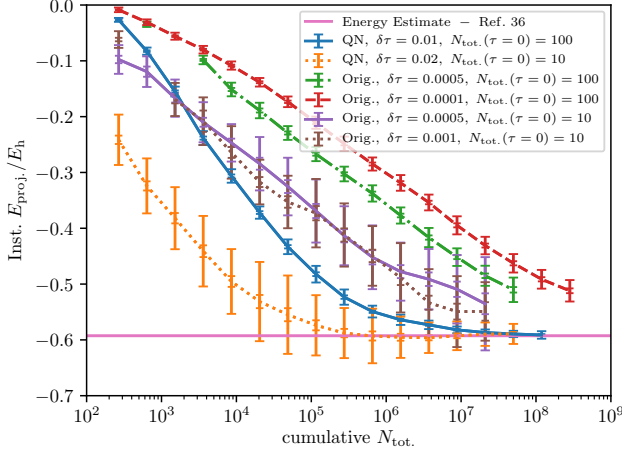


Figure 2: Convergence of the instantaneous projected energy as a function of cumulative number of Monte Carlo particles $N_{\text{tot.}}$ as cost measure for the 3D UEG with 1850 spinorbitals, 14 electrons, and $r_s = 0.5a_0$ in FCIQMC. The instantaneous projected energy was binned with respect to the cumulative particle number and the bin means calculated. Each calculations was done at least 20 times in independent runs and the means of those bin means are shown with their standard deviations and standard errors as outer and inner error bars respectively, placed at the number of cumulative particles that is at the middle of the bin. Not every data point was determined by the same number of independent bins. Calculations here were stopped pre-maturely and could have continued, so the end of a curve does not imply that the memory was full. The estimate for the true energy using (initiator) FCIQMC was taken from Ref. 36. Twice its error is shown in the line spread but it is too small to be visible. $N_{\text{tot.}}(\tau = 0)$ is the initial population. $\rho = 1.0$, $\delta\epsilon \approx 11.8E_h$, $\Delta_v = \delta\epsilon$ and the shift was not varied.

lation was then stopped (and the last iteration printed disregarded). For clarity, only the standard errors are shown this time as errorbars. One of the fastest converging curves each for each propagation run at $M = 1850$ is shown as well for direct comparison. In terms of convergence, the quasi-Newton propagation does not appear to be strongly affected by the increase in system size. However, the original propagation converges slower, not being able to contain the spawns in the given — fixed — spawn array. The original propagation therefore either requires more memory or has to lower the time

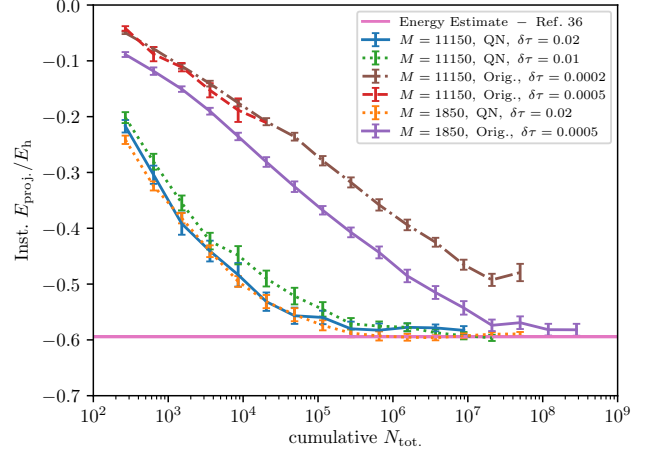


Figure 3: Convergence of the instantaneous projected energy as a function of cumulative number of Monte Carlo particles $N_{\text{tot.}}$ as cost measure for the 3D UEG with $M = 11150$ spinorbitals, 14 electrons, and $r_s = 0.5a_0$ in FCIQMC. The instantaneous projected energy was binned with respect to the cumulative particle number and the bin means calculated. Each calculations was done at least 20 times in independent runs and the means of those bin means are shown with their standard errors as error bars respectively (unlike figure 2, standard deviations are not shown), placed at the number of cumulative particles that is at the middle of the bin. Not every data point was determined by the same number of independent bins. Unlike in figure 2, calculations here were only stopped pre-maturely if the array containing the spawned particles was full and the last printed iteration ignored, except for the quasi-Newton propagation shown for comparison run at 1850 spinorbitals. The calculations for the original propagation at 1850 spinorbitals were rerun. Two estimates for the true energy using (initiator) FCIQMC, taken from Ref. 36, are shown; the energy at 4218 spinorbitals and the complete basis set extrapolated limit. However, they cannot be distinguished within the thickness of the horizontal line. Twice their error is shown respectively in the line spread but it is too small to be visible. $N_{\text{tot.}}(\tau = 0)$, the initial population, was 10. $\rho = 1.0$, $\delta\epsilon \approx 11.8E_h$, $\Delta_v = \delta\epsilon$ and the shift was not varied.

step which in turn, as shown by figure 2, decreases the rate of convergence. Considering that the orbital Fock value increases for added sets of spinorbitals, the stabilising behaviour of quasi-Newton was to be expected by consider-

ing that the spawn probability effectively is divided by the difference in the sum of Fock energies to the reference sum. Provided there is an adequate range in Fock energies, quasi-Newton therefore enables faster convergence rates — especially in larger systems.

5 Application to Cr₂

Finally, the quasi-Newton propagation was tested on an archetypical quantum chemistry problem, the chromium dimer, at a bond length of 1.5 Å. The basis set considered is Ahlrichs’ SV⁶⁰ where first a CAS of 24 electrons correlated in 30 spatial orbitals was applied and then the full system was studied with initiator FCIQMC. The Hartree–Fock orbitals and their integrals were evaluated with the Psi4 code.^{69,70} The weighted heat-bath excitation generator²⁷ (adapted⁴⁸) has been used. Again, floating-point amplitudes^{46,68} were employed with a spawn cutoff of 0.01. Booth et al.²² have previously applied FCIQMC to the chromium dimer with a CAS and DMRG results exist for both smaller CAS^{71–73} and full⁷³ system, also in Ahlrich’s SV basis^{60,4}. For the smaller CAS

⁴Refs. 72 and 22 state that they have used Ahlrich’s SV(P) or SVP basis set. In summary, given that their results agree very well with ours, we conclude that we most likely used the same, SV basis set, details given here. The basis we used (Ahlrich’s SV basis set) can be found at EMSL Basis Set Exchange Library, <https://bse.pnl.gov/bse/portal> [accessed 22.05.2019], under “Ahlrichs VDZ” and selecting “Cr” as the element. It has {63311/53/41} functions.⁶⁰ SV(P)/SVP then contains a polarizing p function (coefficients 0.1206750 and 1.0000000) as well and that basis set can be found under “Ahlrichs pVDZ”. The Hartree–Fock, CCSD and CCSD(T) energies in a CAS of 24 electrons in 30 orbitals (freezing the lowest occupied orbitals) were compared using the Psi4 code. The Hartree–Fock was -2085.57297 E_h in the SV basis and -2085.60285 E_h in the SV(P)/SVP basis. Our full active space SV CCSD(T) energy, -2086.39864 E_h , agrees with Olivares-Amaya et al.⁷³ In this section, the correlation energies of other studies were calculated by subtracting the Hartree–Fock energy in a SV basis (no polarising p) off the total energy quoted in the various studies. The difference in correlation energies between the SV and the SV(P)/SVP basis sets with respect to the SV Hartree–Fock energy in this (24e, 30o) CAS was -0.03 and -0.05 for CCSD and CCSD(T) respectively. This difference is an order of

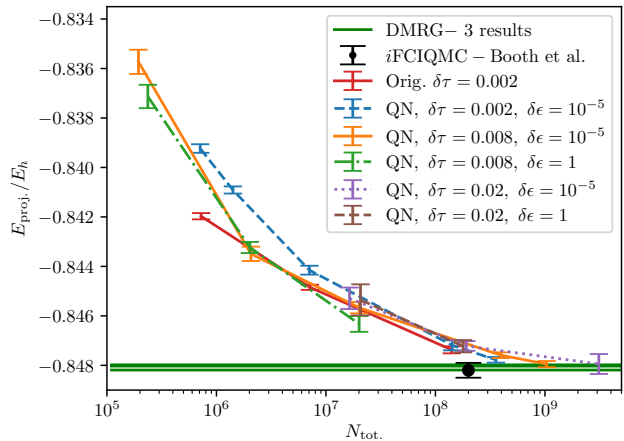


Figure 4: Initiator curve of Cr₂ in a (24 electrons, 30 orbitals) active space in SV basis⁶⁰ at a bond length of 1.5 Å. Three DMRG results^{71–73} are shown with horizontal lines. An initiator curve point from Booth et al.²² is included. $\Delta_v = 1$, $\rho = 1$ here.

system, figure 4 shows various initiator convergence curves, displaying energy as a function of population size, for quasi-Newton and original propagation. The quasi-Newton propagation was tested at $\delta\tau = 0.002, 0.008$ and 0.02 , whereas the original was only stable or did not converge very slowly at $\delta\tau = 0.002$ out of these time steps (given the set initial population etc.). The range of the result by Booth et al.²² is shown. Reblocking analysis was used to estimate errors on quoted energy values.⁷⁴ All initiator curves tend to this result and the threshold $\delta\epsilon$ did not seem to have a noticeable effect.

Convergence of the full all-electron system with a Hilbert space size of 10^{22} was then studied with initiator FCIQMC for a particular target population comparing quasi-Newton to original propagation (figure 5). In figure 5, the convergence of original (at $\delta\tau = 0.0007$) and quasi-Newton propagation defined as the point of overlap with the expected value is comparable. However, the quasi-Newton propagation is slightly faster convergent, even according to that definition, and the cost to get within $\pm 0.005 E_h$, even if not stable, is significantly less costly than with the original propagation.

magnitude larger than energy differences to those studies in this chromium investigation here. We therefore concluded that the basis set used was SV in Refs. 72 and 22 as well.

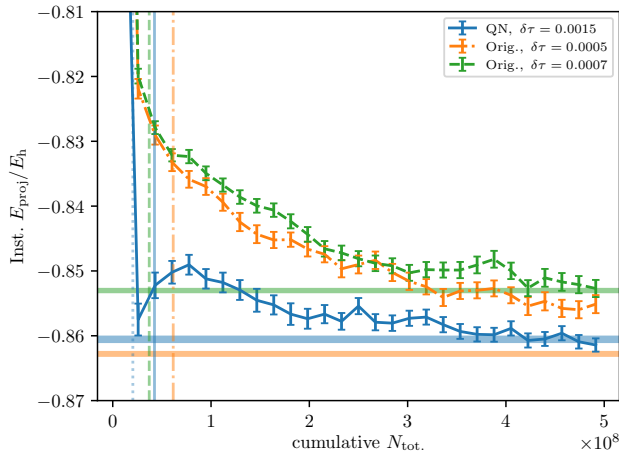


Figure 5: Convergence of instantaneous projected energy in the all-electron chromium dimer in the SV basis⁶⁰ at a bond length of 1.5Å of quasi-Newton (QN) and original propagation at a target population of 5×10^5 (population where shift starts varying) and initial population of 100 using initiator approximation. The QN results were run with $\rho = 0$ up to iteration 5000 ($\delta\tau = 0.0015$) and then set to $\rho = 1$, always using $\Delta_v = 1$ and $\delta\epsilon = 10^{-5}$. The instantaneous projected energy was binned with respect to the cumulative particle number and the bin means calculated. Each calculations was done at least 100 times in independent runs and the means of those bin means are shown with their standard errors as error bars, placed at the number of cumulative particles that is at the middle of the bin. Only calculations where the inst. $E_{\text{proj.}} < 0.1$ and $> -3.8E_h$ always were included. The horizontal lines (least negative $E_{\text{proj.}}$ Orig. at $\delta\tau = 0.0007$, then QN and most negative $E_{\text{proj.}}$ is Orig. at $\delta\tau = 0.0005$) indicate the mean $E_{\text{proj.}}$ and its error found by taking the mean energy of all calculations of that type with at least 5×10^5 iterations. The left most vertical shows when ρ was changed in the QN calculation and the others show when the shift was allowed to vary in the respective calculation. The vertical lines do not show error bars.

An initiator quasi-Newton study with populations up to just above 10^9 was done and a function of the form $a + bx^{-c}$ was fitted to the data set. The determined convergence value is $-0.8717(3) E_h$ which agrees with DMRG,⁷³ $-0.871813 E_h$. The maximum number of particles is of order 10^9 , a factor of 10^{13} reduction from the complete Hilbert space. As with the smaller CAS study, this shows that FCIQMC with quasi-Newton propagation gives reliable energies.

6 Conclusion

We have shown that the quasi-Newton propagation introduced here (applicable to both CCMC and FCIQMC) can accelerate the convergence of the (instantaneous) projected energy compared to the original propagation, especially in large systems with a wider range in orbital energies. It scales more favourably ($\mathcal{O}(1)$ instead of $\mathcal{O}(N_{\text{el.}})$) than the Jacobi propagation while having a comparable benefit. In conjunction with an excitation generator that does not scale with system size, such as the *heat bath Power Pitzer ref.* excitation generator⁴⁸ in the case of CCMC, not adding extra scaling to the algorithm is important in large electronic systems. Using the quasi-Newton propagation, we quoted the first (initiator) FCIQMC result on the chromium dimer in the full SV basis set.⁶⁰

Acknowledgement The open-source HANDE code³⁹ was used for stochastic and FCI calculations and Matplotlib⁷⁵ for figures. We thank Dr. Nick Blunt and Mr. Bang Huynh for helpful conversations. Further information and the research data including (a link to) the deterministic propagation code will be available at <https://doi.org/10.17863/CAM.40122> after acceptance. Before then, please contact the authors for access. V.A.N. would like to acknowledge the EPSRC Centre for Doctoral Training in Computational Methods for Materials Science for funding under grant number EP/L015552/1 and the Cambridge Philosophical Society for a studentship. A.J.W.T. acknowledges the Royal Society for a University Research Fellowship under grants

UF110161 and UF160398. This work used the ARCHER UK National Supercomputing Service (<http://www.archer.ac.uk>) and the UK Research Data Facility (<http://www.archer.ac.uk/documentation/rdf-guide>) under ARCHER leadership grant e507.

References

- (1) Bartlett, R. J.; Musiał, M. Coupled-cluster theory in quantum chemistry. *Rev. Mod. Phys.* **2007**, *79*, 291–352.
- (2) Lynch, B. J.; Truhlar, D. G. Robust and Affordable Multicoefficient Methods for Thermochemistry and Thermochemical Kinetics: The MCCM/3 Suite and SAC/3. *J. Phys. Chem. A* **2003**, *107*, 3898–3906.
- (3) Al-Hamdani, Y. S.; Alfè, D.; von Lilienfeld, O. A. et al. Water on BN doped benzene: A hard test for exchange-correlation functionals and the impact of exact exchange on weak binding. *J. Chem. Phys.* **2014**, *141*, 18C530.
- (4) Veit, M.; Jain, S. K.; Bonakala, S. et al. Equation of State of Fluid Methane from First Principles with Machine Learning Potentials. *J. Chem. Theory Comput.* **2019**, *15*, 2574–2586.
- (5) Yang, J.; Hu, W.; Usvyat, D. et al. Ab initio determination of the crystalline benzene lattice energy to sub-kilojoule/mole accuracy. *Science (80-.)*. **2014**, *345*, 640–643.
- (6) Mostaani, E.; Drummond, N. D.; Fal’ko, V. I. Quantum Monte Carlo calculation of the binding energy of bilayer graphene. *Phys. Rev. Lett.* **2015**, *115*, 115501.
- (7) Gruber, T.; Liao, K.; Tsatsoulis, T. et al. Applying the Coupled-Cluster Ansatz to Solids and Surfaces in the Thermodynamic Limit. *Phys. Rev. X* **2018**, *8*, 021043.
- (8) El-Azhary, A. A coupled-cluster study of the structure and vibrational spectra of pyrazole and imidazole. *Spectrochim. Acta Part A Mol. Biomol. Spectrosc.* **2003**, *59*, 2009–2025.
- (9) Christiansen, O. Vibrational coupled cluster theory. *J. Chem. Phys.* **2004**, *120*, 2149–2159.
- (10) Yuwono, S. H.; Magoulas, I.; Shen, J. et al. Application of the coupled-cluster CC(P ; Q) approaches to the magnesium dimer. *Mol. Phys.* **2019**, *117*, 1486–1506.
- (11) Shavitt, I. In *Methods Electron. Struct. Theory*; Schaefer, H. F., Ed.; Springer US: Boston, MA, 1977; pp 189–275.
- (12) Cremer, D. From configuration interaction to coupled cluster theory: The quadratic configuration interaction approach. *Wiley Interdiscip. Rev. Comput. Mol. Sci.* **2013**, *3*, 482–503.
- (13) Coester, F.; Kümmel, H. Short-range correlations in nuclear wave functions. *Nucl. Phys.* **1960**, *17*, 477–485.
- (14) Čížek, J. On the correlation problem in atomic and molecular systems. Calculation of wavefunction components in Ursell-type expansion using quantum-field theoretical methods. *J. Chem. Phys.* **1966**, *45*, 4256–4266.
- (15) Čížek, J.; Paldus, J. Correlation problems in atomic and molecular systems III. Rederivation of the coupled-pair many-electron theory using the traditional quantum chemical methodst. *Int. J. Quantum Chem.* **1971**, *5*, 359–379.
- (16) Kohn, W.; Sham, L. J. Self-Consistent Equations Including Exchange and Correlation Effects. *Phys. Rev.* **1965**, *140*, A1133–A1138.
- (17) Hohenberg, P.; Kohn, W. Inhomogeneous Electron Gas. *Phys. Rev.* **1964**, *136*, B864–B871.

- (18) Foulkes, W. M. C.; Mitas, L.; Needs, R. J. et al. Quantum Monte Carlo simulations of solids. *Rev. Mod. Phys.* **2001**, *73*, 33–83.
- (19) Raghavachari, K.; Trucks, G. W.; Pople, J. A. et al. A fifth-order perturbation comparison of electron correlation theories. *Chem. Phys. Lett.* **1989**, *157*, 479–483.
- (20) Booth, G. H.; Thom, A. J. W.; Alavi, A. Fermion Monte Carlo without fixed nodes: A game of life, death, and annihilation in Slater determinant space. *J. Chem. Phys.* **2009**, *131*, 054106.
- (21) Thom, A. J. W. Stochastic Coupled Cluster Theory. *Phys. Rev. Lett.* **2010**, *105*, 263004.
- (22) Booth, G. H.; Smart, S. D.; Alavi, A. Linear-scaling and parallelisable algorithms for stochastic quantum chemistry. *Mol. Phys.* **2014**, *112*, 1855–1869.
- (23) Spencer, J. S.; Neufeld, V. A.; Vigor, W. A. et al. Large scale parallelization in stochastic coupled cluster. *J. Chem. Phys.* **2018**, *149*, 204103.
- (24) Booth, G. H.; Cleland, D.; Thom, A. J. W. et al. Breaking the carbon dimer: The challenges of multiple bond dissociation with full configuration interaction quantum Monte Carlo methods. *J. Chem. Phys.* **2011**, *135*, 084104.
- (25) Cleland, D.; Booth, G. H.; Overy, C. et al. Taming the First-Row Diatomics: A Full Configuration Interaction Quantum Monte Carlo Study. *J. Chem. Theory Comput.* **2012**, *8*, 4138–4152.
- (26) Daday, C.; Smart, S.; Booth, G. H. et al. Full Configuration Interaction Excitations of Ethene and Butadiene: Resolution of an Ancient Question. *J. Chem. Theory Comput.* **2012**, *8*, 4441–4451.
- (27) Holmes, A. A.; Changlani, H. J.; Umrigar, C. J. Efficient Heat-Bath Sampling in Fock Space. *J. Chem. Theory Comput.* **2016**, *12*, 1561–1571.
- (28) Sharma, S.; Yanai, T.; Booth, G. H. et al. Spectroscopic accuracy directly from quantum chemistry: Application to ground and excited states of beryllium dimer. *J. Chem. Phys.* **2014**, *140*, 104112.
- (29) Veis, L.; Antalík, A.; Legeza, Ö. et al. The Intricate Case of Tetramethyleneethane: A Full Configuration Interaction Quantum Monte Carlo Benchmark and Multireference Coupled Cluster Studies. *J. Chem. Theory Comput.* **2018**, *14*, 2439–2445.
- (30) Samanta, P. K.; Blunt, N. S.; Booth, G. H. Response Formalism within Full Configuration Interaction Quantum Monte Carlo: Static Properties and Electrical Response. *J. Chem. Theory Comput.* **2018**, *14*, 3532–3546.
- (31) Spencer, J. S.; Thom, A. J. W. Developments in stochastic coupled cluster theory: The initiator approximation and application to the uniform electron gas. *J. Chem. Phys.* **2016**, *144*, 084108.
- (32) Martin, R. M. *Electron. Struct.*; Cambridge University Press: Cambridge, 2004; pp 100–118.
- (33) Shepherd, J. J.; Booth, G.; Grüneis, A. et al. Full configuration interaction perspective on the homogeneous electron gas. *Phys. Rev. B* **2012**, *85*, 081103.
- (34) Shepherd, J. J.; Grüneis, A. Many-body quantum chemistry for the electron gas: Convergent perturbative theories. *Phys. Rev. Lett.* **2013**, *110*, 226401.
- (35) Shepherd, J. J. Communication: Convergence of many-body wave-function expansions using a plane-wave basis in the thermodynamic limit. *J. Chem. Phys.* **2016**, *145*, 031104.
- (36) Neufeld, V. A.; Thom, A. J. W. A study of the dense uniform electron gas with high

- orders of coupled cluster. *J. Chem. Phys.* **2017**, *147*, 194105.
- (37) Luo, H.; Alavi, A. Combining the Transcorrelated Method with Full Configuration Interaction Quantum Monte Carlo: Application to the Homogeneous Electron Gas. *J. Chem. Theory Comput.* **2018**, *14*, 1403–1411.
- (38) Booth, G. H.; Grüneis, A.; Kresse, G. et al. Towards an exact description of electronic wavefunctions in real solids. *Nature* **2013**, *493*, 365–370.
- (39) Spencer, J. S.; Blunt, N. S.; Choi, S. et al. The HANDE-QMC Project: Open-Source Stochastic Quantum Chemistry from the Ground State Up. *J. Chem. Theory Comput.* **2019**, *15*, 1728–1742.
- (40) Booth, G. H.; Chan, G. K.-L. Communication: Excited states, dynamic correlation functions and spectral properties from full configuration interaction quantum Monte Carlo. *J. Chem. Phys.* **2012**, *137*, 191102.
- (41) Ten-no, S. Stochastic determination of effective Hamiltonian for the full configuration interaction solution of quasi-degenerate electronic states. *J. Chem. Phys.* **2013**, *138*, 164126.
- (42) Humeniuk, A.; Mitrić, R. Excited states from quantum Monte Carlo in the basis of Slater determinants. *J. Chem. Phys.* **2014**, *141*, 194104.
- (43) Blunt, N. S.; Smart, S. D.; Booth, G. H. et al. An excited-state approach within full configuration interaction quantum Monte Carlo. *J. Chem. Phys.* **2015**, *143*, 134117.
- (44) Blunt, N. S.; Booth, G. H.; Alavi, A. Density matrices in full configuration interaction quantum Monte Carlo: Excited states, transition dipole moments, and parallel distribution. *J. Chem. Phys.* **2017**, *146*, 244105.
- (45) Cleland, D.; Booth, G. H.; Alavi, A. Communications: Survival of the fittest: Accelerating convergence in full configuration-interaction quantum Monte Carlo. *J. Chem. Phys.* **2010**, *132*, 041103.
- (46) Petruzielo, F. R.; Holmes, A. A.; Changlani, H. J. et al. Semistochastic Projector Monte Carlo Method. *Phys. Rev. Lett.* **2012**, *109*, 230201.
- (47) Blunt, N. S.; Smart, S. D.; Kersten, J. A. F. et al. Semi-stochastic full configuration interaction quantum Monte Carlo: Developments and application. *J. Chem. Phys.* **2015**, *142*, 184107.
- (48) Neufeld, V. A.; Thom, A. J. W. Exciting Determinants in Quantum Monte Carlo: Loading the Dice with Fast, Low-Memory Weights. *J. Chem. Theory Comput.* **2019**, *15*, 127–140.
- (49) Scott, C. J. C.; Thom, A. J. W. Stochastic coupled cluster theory: Efficient sampling of the coupled cluster expansion. *J. Chem. Phys.* **2017**, *147*, 124105.
- (50) Scott, C. J. C.; Di Remigio, R.; Crawford, T. D. et al. Diagrammatic Coupled Cluster Monte Carlo. *J. Phys. Chem. Lett.* **2019**, *10*, 925–935.
- (51) Helgaker, T.; Jørgensen, P.; Olsen, J. *Mol. Electron. Theory*; John Wiley & Sons, Ltd: Chichester, UK, 2000; pp 648–723.
- (52) Blunt, N. S.; Thom, A. J. W.; Scott, C. J. C. Preconditioning and Perturbative Estimators in Full Configuration Interaction Quantum Monte Carlo. *J. Chem. Theory Comput.* **2019**, *15*, 3537–3551.
- (53) Davidson, E. R. The iterative calculation of a few of the lowest eigenvalues and corresponding eigenvectors of large real-symmetric matrices. *J. Comput. Phys.* **1975**, *17*, 87–94.
- (54) Zhang, T.; Evangelista, F. A. A Deterministic Projector Configuration Interaction

- Approach for the Ground State of Quantum Many-Body Systems. *J. Chem. Theory Comput.* **2016**, *12*, 4326–4337.
- (55) Schwarz, L. R.; Alavi, A.; Booth, G. H. Projector Quantum Monte Carlo Method for Nonlinear Wave Functions. *Phys. Rev. Lett.* **2017**, *118*, 176403.
- (56) Sabzevari, I.; Sharma, S. Improved Speed and Scaling in Orbital Space Variational Monte Carlo. *J. Chem. Theory Comput.* **2018**, *14*, 6276–6286.
- (57) Otis, L.; Neuscamman, E. Complementary first and second derivative methods for ansatz optimization in variational Monte Carlo. *Phys. Chem. Chem. Phys.* **2019**, *21*, 14491–14510.
- (58) Deustua, J. E.; Shen, J.; Piecuch, P. Converging High-Level Coupled-Cluster Energetics by Monte Carlo Sampling and Moment Expansions. *Phys. Rev. Lett.* **2017**, *119*, 223003.
- (59) Deustua, J. E.; Magoulas, I.; Shen, J. et al. Communication: Approaching exact quantum chemistry by cluster analysis of full configuration interaction quantum Monte Carlo wave functions. *J. Chem. Phys.* **2018**, *149*, 151101.
- (60) Schäfer, A.; Horn, H.; Ahlrichs, R. Fully optimized contracted Gaussian basis sets for atoms Li to Kr. *J. Chem. Phys.* **1992**, *97*, 2571–2577.
- (61) Davidson, E. R.; Thompson, W. J. Monster Matrices: Their Eigenvalues and Eigenvectors. *Comput. Phys.* **1993**, *7*, 519.
- (62) Shepherd, J. J. A Quantum Chemical Perspective on the Homogeneous Electron Gas. Ph.D. thesis, University of Cambridge, 2013.
- (63) Schoof, T.; Groth, S.; Vorberger, J. et al. Ab Initio Thermodynamic Results for the Degenerate Electron Gas at Finite Temperature. *Phys. Rev. Lett.* **2015**, *115*, 130402.
- (64) Fraser, L. M.; Foulkes, W. M. C.; Rajagopal, G. et al. Finite-size effects and Coulomb interactions in quantum Monte Carlo calculations for homogeneous systems with periodic boundary conditions. *Phys. Rev. B* **1996**, *53*, 1814–1832.
- (65) Trivedi, N.; Ceperley, D. M. Ground-state correlations of quantum antiferromagnets: A Green-function Monte Carlo study. *Phys. Rev. B* **1990**, *41*, 4552–4569.
- (66) Franklin, R. S. T.; Spencer, J. S.; Zocante, A. et al. Linked coupled cluster Monte Carlo. *J. Chem. Phys.* **2016**, *144*, 044111.
- (67) Smart, S. D.; Booth, G. H.; Alavi, A. Excitation generation in full configuration interaction quantum Monte Carlo based on Cauchy-Schwarz distributions. *unpublished*
- (68) Overy, C.; Booth, G. H.; Blunt, N. S. et al. Unbiased reduced density matrices and electronic properties from full configuration interaction quantum Monte Carlo. *J. Chem. Phys.* **2014**, *141*, 244117.
- (69) Turney, J. M.; Simmonett, A. C.; Parrish, R. M. et al. Psi4: an open-source ab initio electronic structure program. *Wiley Interdiscip. Rev. Comput. Mol. Sci.* **2012**, *2*, 556–565.
- (70) Parrish, R. M.; Burns, L. A.; Smith, D. G. A. et al. Psi4 1.1: An Open-Source Electronic Structure Program Emphasizing Automation, Advanced Libraries, and Interoperability. *J. Chem. Theory Comput.* **2017**, *13*, 3185–3197.
- (71) Kurashige, Y.; Yanai, T. High-performance ab initio density matrix renormalization group method: Applicability to large-scale multireference problems for metal compounds. *J. Chem. Phys.* **2009**, *130*, 234114.
- (72) Sharma, S.; Chan, G. K.-L. Spin-adapted density matrix renormalization group al-

gorithms for quantum chemistry. *J. Chem. Phys.* **2012**, *136*, 124121.

- (73) Olivares-Amaya, R.; Hu, W.; Nakatani, N. et al. The ab-initio density matrix renormalization group in practice. *J. Chem. Phys.* **2015**, *142*, 034102.
- (74) Flyvbjerg, H.; Petersen, H. G. Error estimates on averages of correlated data. *J. Chem. Phys.* **1989**, *91*, 461–466.
- (75) Hunter, J. D. Matplotlib: A 2D Graphics Environment. *Comput. Sci. Eng.* **2007**, *9*, 90–95.

Graphical TOC Entry

